



Combining multigrid and wavelet ideas to construct more efficient multiscale algorithms for the solution of Poisson's equation

Stefan Goedecker, Claire Chauvin

► To cite this version:

Stefan Goedecker, Claire Chauvin. Combining multigrid and wavelet ideas to construct more efficient multiscale algorithms for the solution of Poisson's equation. *Journal of Theoretical and Computational Chemistry*, 2003, 2 (2), pp.483-495. 10.1142/S021963360300063X . hal-00450034

HAL Id: hal-00450034

<https://hal.science/hal-00450034>

Submitted on 25 Jan 2010

HAL is a multi-disciplinary open access archive for the deposit and dissemination of scientific research documents, whether they are published or not. The documents may come from teaching and research institutions in France or abroad, or from public or private research centers.

L'archive ouverte pluridisciplinaire **HAL**, est destinée au dépôt et à la diffusion de documents scientifiques de niveau recherche, publiés ou non, émanant des établissements d'enseignement et de recherche français ou étrangers, des laboratoires publics ou privés.

Combining multigrid and wavelet ideas to construct more efficient multiscale algorithms for the solution of Poisson's equation

Stefan Goedecker, Claire Chauvin

Département de recherche fondamentale sur la matière condensée,
SP2M/L_Sim, CEA-Grenoble, 38054 Grenoble cedex 9, France

1 Abstract

It is shown how various ideas that are well established for the solution of Poisson's equation using plane wave and Multigrid methods can be incorporated into the wavelet context. The combination of wavelet concepts and multigrid techniques turns out to be particularly fruitful. We propose a modified multigrid V cycle scheme that is not only much simpler, but also more efficient than the standard V cycle. Whereas in the traditional V cycle the residue is passed to the coarser grid levels, this new scheme does not require the calculation of a residue. Instead it works with copies of the charge density on the different grid levels that were obtained from the underlying charge density on the finest grid by wavelet transformations. This scheme is not limited to the pure wavelet setting, where it is faster than the preconditioned conjugate gradient method, but equally well applicable for finite difference discretizations of Poisson's equation.

2 Introduction

Poisson's equation

$$\nabla^2 V(\mathbf{r}) = -4\pi\rho(\mathbf{r}) \quad (1)$$

is the basic equation for electrostatic problems. As such it plays an important role in a large variety of scientific and technological problems. The solution of the differential equation (Eq. 1) can be written as an integral equation

$$V(\mathbf{r}) = \int \frac{\rho(\mathbf{r}')}{|\mathbf{r} - \mathbf{r}'|} \quad (2)$$

Gravitational problems are based on exactly the same equations as the electrostatic problem, but we will use in this article the language of electrostatics, i.e. we will refer to $\rho(\mathbf{r})$ as a charge density. The most efficient numerical approaches for the solution of electrostatic problems are based on (Eq 1) rather than (Eq. 2). However preconditioning steps found in these methods can be considered as approximate solutions of (Eq. 2). The fact that the Green's function $\frac{1}{|\mathbf{r}-\mathbf{r}'|}$ is of long range makes the numerical solution of Poisson's equation difficult, since it implies that a charge density at a point \mathbf{r}' will have a non-negligible influence on the potential $V(\mathbf{r})$ at a point \mathbf{r} far away. A naive implementation of (Eq. 2) would therefore have a quadratic scaling. It comes however to our help, that the potential arising from a charge distribution far away is slowly varying

and does not depend on the details of the charge distribution. All efficient algorithms for solving electrostatic problems are therefore based on a hierarchical multiscale treatment. On the short length scales the rapid variations of the potential due to the exact charge distribution of close by sources of charge are treated, on the large length scales the slow variation due to some smoothed charge distribution of far sources is accounted for. Since the number of degrees of freedom decreases rapidly with increasing length scales, one can obtain algorithms with linear or nearly linear scaling. In the following, we will briefly summarize how this hierarchical treatment is implemented in the standard algorithms

- Fourier Analysis:

If the charge density is written in its Fourier representation

$$\rho(\mathbf{r}) = \sum_{\mathbf{K}} \rho_{\mathbf{K}} e^{i\mathbf{K}\mathbf{r}}$$

the different length scales that are in this case given by $\lambda = \frac{2\pi}{K}$ decouple entirely and the Fourier representation of the potential is given by

$$V(\mathbf{r}) = \sum_{\mathbf{K}} \frac{\rho_{\mathbf{K}}}{K^2} e^{i\mathbf{K}\mathbf{r}} \quad (3)$$

The Fourier analysis of the real space charge density necessary to obtain its Fourier components $\rho_{\mathbf{K}}$ and the synthesis of the potential in real space from its Fourier components given by (Eq. 3) can be done with Fast Fourier methods at a cost of $N \log_2(N)$ where N is the number of grid points. The solution of Poisson's equation in a plane wave is thus a divide and conquer approach where the division is into the single Fourier components.

- Multigrid methods (MG):

Trying to solve Poisson's equation by any relaxation or iterative method (such as conjugate gradient) on the fine grid on which one finally wants to have the solution leads to a number of iterations that increases strongly with the size of the grid. The reason for this is that on a grid with a given spacing h one can efficiently treat Fourier components with a wavelength $\lambda = \frac{2\pi}{K}$ that is comparable to the grid spacing h , but the longer wavelength Fourier components converge very slowly. This increase in the number of iterations prevents a straightforward linear scaling solution of (Eq. 1). In the multigrid method, pioneered by A. Brandt [1], one is therefore introducing a hierarchy of grids with a grid spacing that is increasing by a factor of two on each hierarchic level. In contrast to the Fourier method where the charge and the potential are directly decomposed into components characterized by a certain length scale, it is the residue that is passed from the fine grids to the coarse grids in the MG method. The residue corresponds to the charge that would give rise to a potential that is the difference between the exact potential and the approximate potential at the current stage of the iteration.

The solution of partial differential equations in a wavelet basis is typically done by preconditioned iterative techniques [2]. The diagonal preconditioning approach, that is

based on well established plane wave techniques, will be presented in the next section. The section after the next will introduce multigrid for Poisson's equation in a wavelet basis. Even though the fundamental similarities between wavelet and multigrid schemes have been recognized by many workers (such as [3]) this sections contains to the best of our knowledge the first thorough discussion of how both methods can profit from each other.

Within wavelet theory [4] one has two possible representations of a function $f(x)$, a scaling function representation

$$f(x) = \sum_j s_j^{Lmax} \phi_j^{Lmax}(x) \quad (4)$$

and a wavelet representation.

$$f(x) = \sum_j s_j^{Lmin} \phi_j^{Lmin}(x) + \sum_{l=Lmin}^{Lmax} \sum_j d_j^l \psi_j^l(x). \quad (5)$$

In contrast to the scaling function representation, the wavelet representation is a hierarchic representation. The wavelet at the hierarchic level l is related to the mother wavelet ψ by

$$\psi_i^l(x) = \sqrt{2^l} \psi(2^l x - i) \quad (6)$$

The characteristic length scale of a wavelet at resolution level l is therefore proportional to 2^{-l} . A wavelet on a certain level l is a linear combination of scaling functions at the higher resolution level $l+1$

$$\psi_i^l(x) = \sum_{j=-m}^m g_j \phi_{2i+j}^{l+1}(x) \quad (7)$$

Scaling functions at adjacent resolution levels are related by a similar refinement relation

$$\phi_i^l(x) = \sum_{j=-m}^m h_j \phi_{2i+j}^{l+1}(x) \quad (8)$$

and hence also any wavelet at a resolution level l is a linear combination of the highest resolution scaling functions. The so-called fast wavelet transform allows us to transform back and forth between a scaling function and a wavelet representation.

Let us now introduce wavelet representations of the potential and the charge density

$$V(x) = \sum_j V_j^{Lmin} \phi_j^{Lmin}(x) + \sum_{l=Lmin}^{Lmax} \sum_j V_j^l \psi_j^l(x) \quad (9)$$

$$\rho(x) = \sum_j \rho_j^{Lmin} \phi_j^{Lmin}(x) + \sum_{l=Lmin}^{Lmax} \sum_j \rho_j^l \psi_j^l(x) \quad (10)$$

Different levels do not completely decouple, i.e the components on level l , V_j^l , of the exact overall solution do not satisfy the single level Poisson equation

$$\nabla^2 \left(\sum_j V_j^l \psi_j^l(x) \right) \neq -4\pi \left(\sum_j \rho_j^l \psi_j^l(x) \right) \quad (11)$$

within the chosen discretization scheme. This is due to the fact that the wavelets are not perfectly localized in Fourier space, i.e. many frequencies are necessary to synthesize a wavelet. However the amplitude of all these frequencies is clearly peaked at a nonzero characteristic frequency for any wavelet with at least one vanishing moment. From the scaling property (Eq. 6) it follows, that the frequency at which the peak occurs changes by a factor of two on neighboring resolution grids. This suggests that the coupling between the different resolution levels is weak.

In the preceding paragraph we presented the mathematical framework only for the one-dimensional case. The generalization to the 3-dim case is straightforward by using tensor products [4]. Also in the rest of the paper only the one-dimensional form of the mathematical formulas will be presented for reasons of simplicity. It has to be stressed however that all the numerical results were obtained for the three-dimensional case and with periodic boundary conditions.

3 The diagonal preconditioning approach for wavelets

Preconditioning requires finding a matrix with a simple structure that has eigenvalues and eigenvectors that are similar to the ones of the matrix in question [5, 6]. The structure has to be simple in the sense that it allows us to calculate the inverse easily. The simplest and most widely used structure in this respect is the structure of a diagonal matrix. As will be shown a diagonal preconditioning matrix can be found in a wavelet basis set and preconditioned conjugate gradient type methods are then a possible method for the solution of Poisson's equation expressed in differential form (Eq.1).

As one adds successive levels of wavelets to the basis set the largest eigenvalue grows by a factor of 4 for each level. This can easily be understood from Fourier analysis. As one increases the resolution by a factor of 2 (i.e. increases the largest Fourier vector k_{max} by a factor of 2) the largest eigenvalue increases by a factor of 4. This basic scaling property of the eigenvalue spectrum can easily be modeled by a diagonal matrix, where all the diagonal elements are all equal on one resolution level, but increase by a factor of 4 as one goes to a higher resolution level. It is of course clear that all the details of the true spectrum are not reproduced by this approximation. The true spectrum consists of a large number of moderately degenerate eigenvalues. The spectrum of the approximate matrix consists of a few highly degenerate eigenvalues where each eigenvalue has all the scaling functions of one resolution level as its eigenfunctions. The true eigenfunctions are of course mixtures of scaling functions on different resolution levels, but if the wavelet family is well localized in Fourier space the contributions from neighboring resolution levels are weak. The localization in Fourier space increases with the number of vanishing moments [7] and therefore this diagonal preconditioning method works for instance much better for lifted interpolating wavelets than for ordinary interpolating wavelets [8].

Another line of arguments, that shows the weakness of the diagonal preconditioning, is the following. The preconditioning matrix can also be considered to be the diagonal part of the matrix representing the Laplacian. Since the diagonal elements increase by a

factor of 4 on each higher resolution level,

$$\begin{aligned} \int \tilde{\psi}_0^{l+1}(x) \frac{\partial^2}{\partial x^2} \psi_0^{l+1}(x) dx &= 2 \int \tilde{\psi}_0^l(2x) \frac{\partial^2}{\partial x^2} \psi_0^l(2x) dx \\ &= 4 \int \tilde{\psi}_j^l(x) \frac{\partial^2}{\partial x^2} \psi_j^l(x) dx \end{aligned} \quad (12)$$

the spectrum of the matrix has again the correct scaling properties. In the 3-dimensional case there are three different types of wavelets (products of 2 scaling functions and 1 wavelet, products of 1 scaling function and 2 wavelets and products of 3 wavelets). Each type of wavelet gives rise to a different diagonal element, but again all these diagonal elements differ by a factor of 4 on different resolution levels. Because of the weak coupling between different resolution levels discussed above, we expect the matrix elements of the Laplacian involving wavelets at two different resolutions levels to be small. The numerical examination of the matrix elements (Fig. 1) confirms this guess. It also shows that within one resolution level the amplitude of the matrix elements decays rapidly with respect to the distance of the two wavelets and is zero as soon as they do not any more overlap. Nevertheless, some matrix elements coupling nearest neighbor wavelets are not much smaller than the diagonal elements. One also finds a few matrix elements between different resolution levels that are less than one order of magnitude smaller than the one within a single resolution level.

The fact that all off-diagonal matrix elements are neglected in current precondition schemes explains their relatively slow convergence. It amounts to finding an approximate Greens function that is diagonal in a wavelet representation. This is obviously a rather poor approximation. Let us nevertheless stress that this diagonal matrix obtained by inverting a diagonal approximation to the Laplacian is a much more reasonable approximation for preconditioning purposes than the diagonal part of the Greens function. The diagonal part of the Greens function has actually completely different scaling properties. The elements increase by a factor of 2 as one goes to higher resolution levels instead of decreasing by a factor of 4. The multigrid methods to be discussed later include also in an approximative way through Gauss-Seidel relaxations this off-diagonal coupling within each resolution block as well as the coupling between the different resolutions levels.

In the following we will present some numerical results for the solution of the 3-dimensional Poisson equation in a wavelet basis using the diagonal preconditioning approach. All the methods presented in this paper will have the property that the convergence rate is independent of the grid size. We have chosen 64^3 grids for all the numerical examples. The fact that the number of iterations necessary to reach a certain target accuracy is independent of the system size together with the fact that a single iteration involves a cost that is linear with respect to the number of grid points ensures that the Poisson's equation can be solved with overall linear scaling. Whereas we use here only simple equidistant grids, this linear scaling has already been demonstrated with highly adaptive grids in problems that involve many different length scales [8, 9, 10, 11].

The preconditioning step using simply the diagonal is given by

$$\Delta V_j^l = \text{const } 4^{-l} \Delta \rho_j^l \quad (13)$$

In analogy to Eq. 9,10, the $\Delta \rho_j^l$'s are the wavelet coefficients on the l -th resolution level of the residue $\Delta \rho(\mathbf{r}) = \nabla^2 \tilde{V}(\mathbf{r}) + 4\pi \rho(\mathbf{r})$ in a wavelet representation. $\tilde{V}(\mathbf{r})$ is the approximate

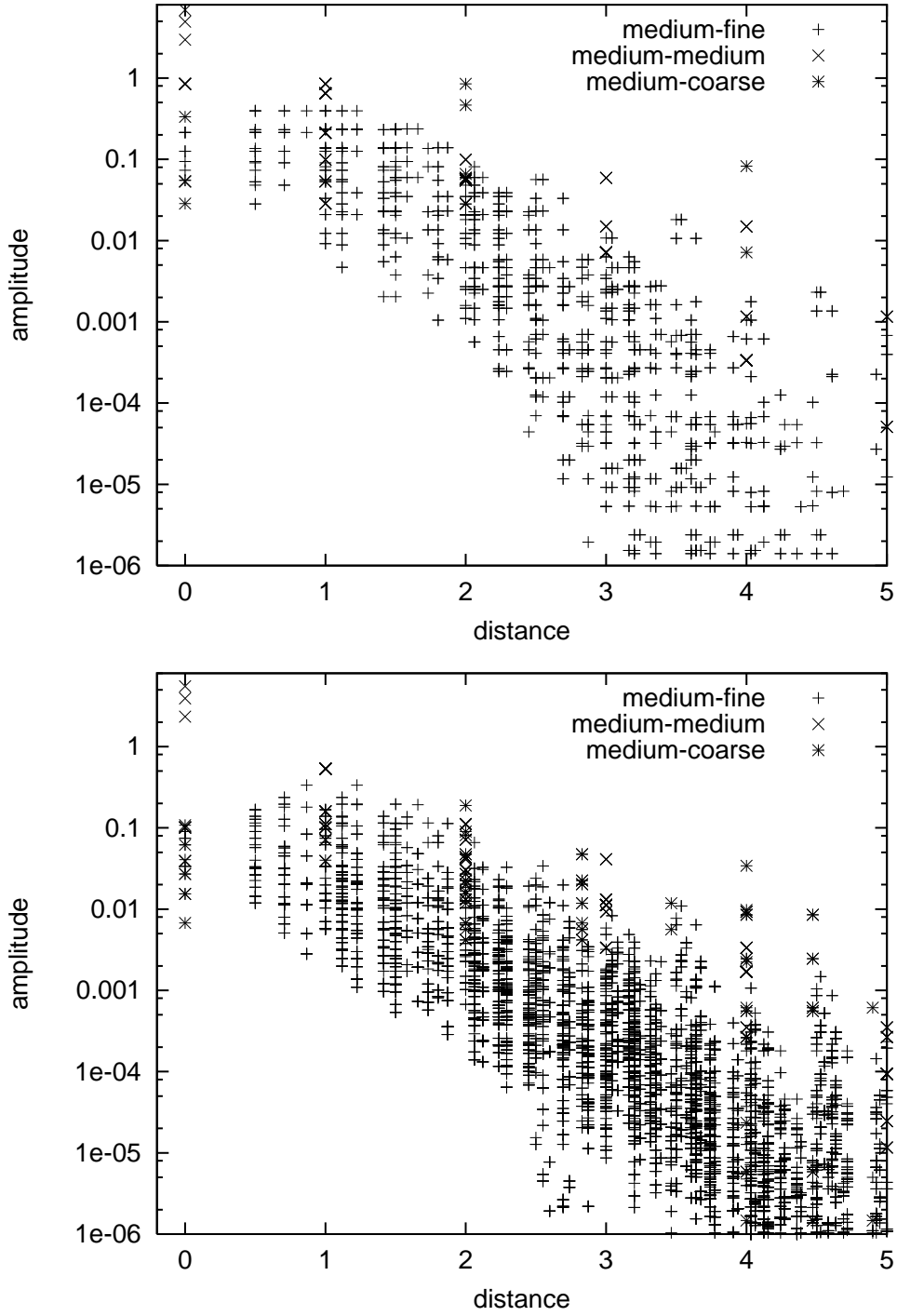


Figure 1: The absolute value of the amplitude of the matrix elements of the Laplacian in a basis of 6-th order interpolating (top panel) and 6-th order lifted interpolating (lower panel) wavelets. Shown are the elements within one resolution block (medium-medium) as well as the elements coupling to a higher resolution (medium-fine) and a lower resolution level (medium-coarse). The distance 1 corresponds to the nearest neighbor distance on the medium resolution level. Because of the better localization in Fourier space of the lifted wavelets, the matrix is more diagonally dominant in the lifted wavelet representation.

solution at a certain iteration of the solution process. The preconditioned residue ΔV is then used to update the approximate potential \tilde{V} . In the case of the preconditioned steepest descent method used here this update simply reads

$$\tilde{V} \leftarrow \tilde{V} + \alpha \Delta V \quad (14)$$

where α is an appropriate step size. As discussed above the constant in (Eq. 13) depends in the three dimensional case upon which type of wavelet is implied since it is the inverse of the Laplace matrix element between two wavelets of this type.

(Fig. 2) shows numerical results for several wavelet families. The slow convergence of the interpolating wavelets is due to the fact that they have a non-vanishing average and therefore a non-vanishing zero Fourier component [8]. Hence they are all localized in Fourier space at the origin instead of being localized around a non-zero frequency. This deficiency can be eliminated by lifting. The Fourier power spectrum of the lifted wavelets tends to zero at the origin with zero slope for the family with two vanishing moments considered here. Lifting the wavelet twice leads to 4 vanishing moments and a even better localization in Fourier space. The improvement in the convergence rate is however only marginal. The higher 8-th order lifted interpolating wavelet is smoother than its 6-th order counterpart and hence better localized in the high frequency part. This also leads to a slightly faster convergence.

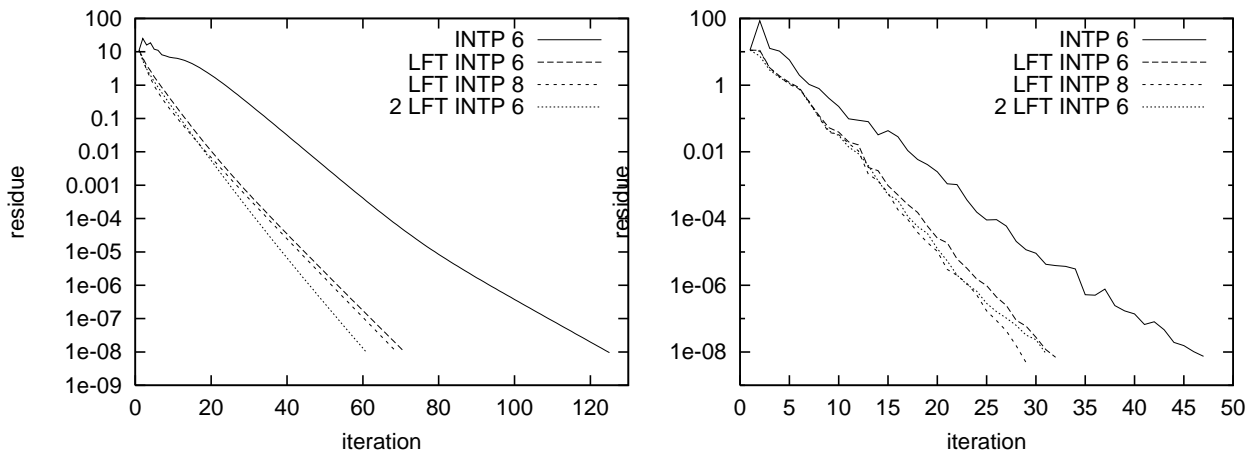


Figure 2: The reduction of the residue during a steepest descent iteration (left hand panel) and a FGMRES iteration (right hand panel) with interpolating and lifted interpolating wavelets.

Combining the diagonal preconditioning (Eq. 13) with a FGMRES convergence accelerator [12] instead of using it within a steepest descent minimization gives a significantly faster convergence. The number of iterations can nearly be cut into half as shown in (Fig 2).

Up to now we have only considered the case where the elements of the matrix representing the Laplacian were calculated within the same wavelet family that was used to

analyze the residue by wavelet transformations to do the preconditioning step. More general schemes can however be implemented. It is not even necessary that the calculation of the Laplacian matrix elements is done in a wavelet basis. One can instead use simple second order finite differences, which in the one-dimensional case are given by

$$\frac{1}{h^2}(-V_{i-1} + 2V_i - V_{i+1}), \quad (15)$$

or some higher order finite differences for the calculation of the matrix elements. The scaling relation (Eq. 12) does not any more hold exactly, but it is fulfilled approximately and the schemes works as well as in the pure wavelet case as is shown in (Fig. 3).

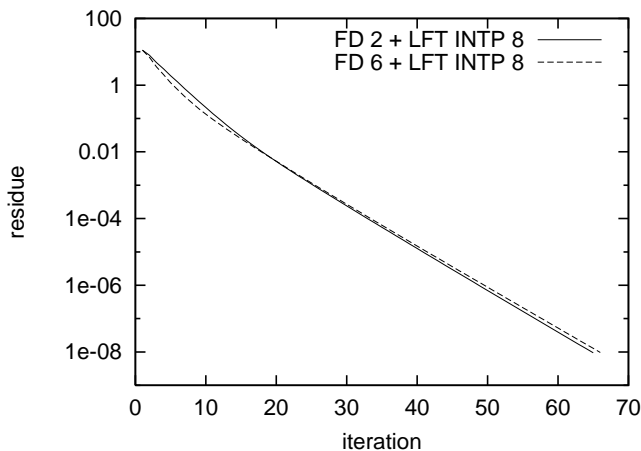


Figure 3: The convergence rate for the case where Poisson's equation is solved with finite differences and 8-th order lifted wavelets are used for the preconditioned steepest descent.

4 The MG approach for wavelets

The aim of this part of the article is twofold. One aspect is how to speed up the convergence of the solution process for Poisson's equation expressed in a wavelet basis set compared to the diagonal preconditioning approach. The other aspect is how to accelerate multigrid schemes by incorporating wavelet concepts. The part therefore begins with a brief review of the multigrid method.

(Fig. 4) schematically shows the algorithm of a standard multigrid V cycle [13, 14]. Even though the scheme is valid in any dimension, a two dimensional setting is suggested by the figure, since the data is represented as squares. Since less data is available on the coarse grids, the squares holding the coarse grid data are increasingly smaller. It has to be stressed that the remarks of the end of the first part remain valid and that in particular all the numerical calculations are 3-dim calculations. The upper half of the figure shows the first part of the V cycle where one goes from the finest grid to the coarsest grid and the lower half the second part where one goes back to the finest grid.

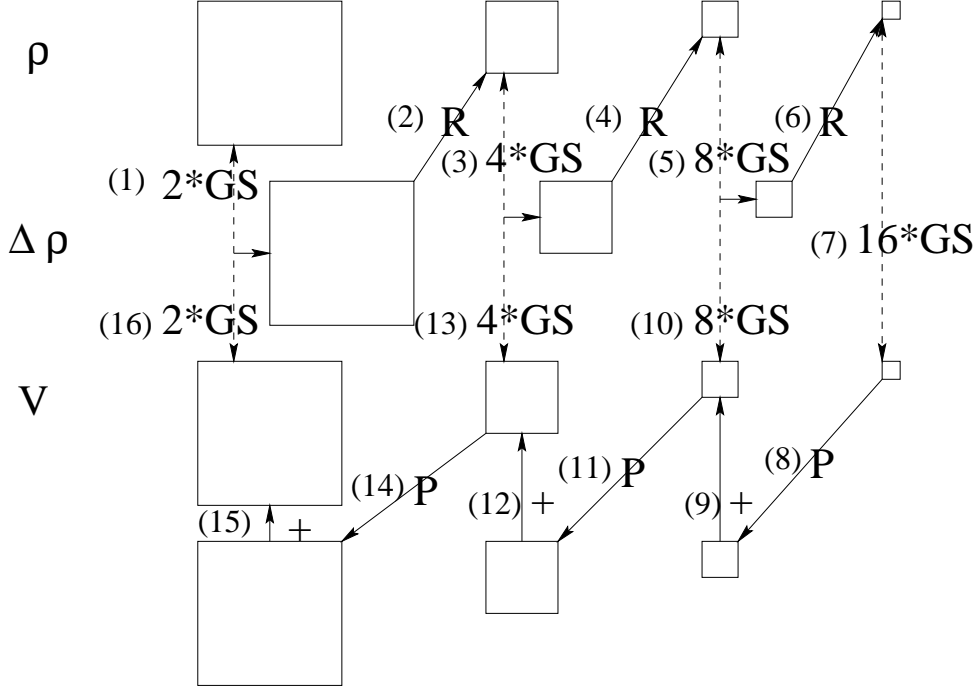


Figure 4: Schematic representation of a multigrid V cycle as described in the text. GS denotes a red-black Gauss-Seidel relaxation, R restriction, P prolongation and + addition of the data sets. The numbering in parentheses gives the ordering of the different steps of the algorithm.

In the first part of the V cycle the potential on all hierarchic grids is improved by a standard red-black Gauss-Seidel relaxation denoted by GS. The GS relaxation reduces the error components of wavelengths λ that are comparable to the grid spacing h very efficiently. In the 3-dimensional case we are considering here, the smoothing factor is .445 (page 74 of ref [13]). Since we use 2 GS relaxations roughly one quarter of the error around the wavelength h survives the relaxations on each level. As a consequence the residue $\Delta\rho$ contains mainly longer wavelengths which then in turn are again efficiently eliminated by the GS relaxations on the coarser grids. Nevertheless, the remaining quarter of the shorter wavelengths surviving the relaxations on the finer grid pollutes the residue on the coarser grid through aliasing effects. Aliasing pollution means that even if the residue on the finer grid would contain only wavelengths around h (and in particular no wavelength around $2h$) the restricted quantity would not be identically zero.

In the second part of the V cycle the solutions obtained by relaxation on the coarse grid are prolonged to the fine grids and added to the existing solutions on each level. Aliasing pollution is again present in the prolongation procedure. Due to the accumulated aliasing errors 2 GS relaxations are again done on each level before proceeding to the next finer level.

To a first approximation the different representations of ρ at the top of (Fig. 4) represent Fourier filtered versions of the real space data set ρ on the finest grid. The large

data set contains all the Fourier components, while the smaller data sets contain only lower and lower frequency parts of ρ . In the 1-dimensional case only the lower half of the spectrum is still dominating when going to the coarse grid, in the 3-dimensional case it is only one eighth of the spectrum. Because of the various aliasing errors described above the Fourier decomposition is however not perfect. Obviously it would be desirable to make this Fourier decomposition as perfect as possible. In the absence of aliasing errors, the GS relaxations would not have to deal with any Fourier components spilling over from higher or lower resolution grids.

Let us now postulate ideal restriction and prolongation operators and discuss their properties. As follows from the discussion above, they should provide for a dyadic decomposition of the Fourier space. Consequently the restriction operator would have to be a perfect low pass filter for the lower half of the spectrum (in the 1-dim case, in the 3-dim case only 1/8 would survive). We will refer to this property in following as frequency separation property. The degree of perfectness can be quantified by the k dependent function

$$S^l(k) = \sqrt{\sum_i (s_i^l)^2 / N} \quad (16)$$

where N is the number of grid points on resolution level l . The k dependence enters through the requirement that the signal s_i^{Lmax} on the finest resolution level is a pure harmonic,

$$s_i^{Lmax} = \exp(I2\pi ki/N) \quad (17)$$

The function $S^l(k)$ for a perfect restriction operator is shown in (Fig 5). Such ideal grid transfer operators have to satisfy a second property, that will be baptized the identity property. The prolongation operator has to bring back exactly onto the finer grid the long wavelength associated with the coarser grid. This can only be true if prolongation followed by a restriction gives the identity. A third desirable property would be that the coarsed charge density represents as faithfully as possible the significant features of the original charge density. In particular the coarsed charge density should have the same multipoles and most importantly the same monopole. The conservation of the monopole just means that the total charge is identical on all grid levels. This third property will be called the multipole conservation property in the following.

With the ideal grid transfer operators, the solution of Poisson's equation would be a divide and conquer approach in Fourier space and it could be done with a single V cycle with a moderate number of GS relaxations on each resolution level. In contrast to a solution in a plane wave basis the division would not be into single Fourier components but into dyadic parts of the Fourier spectrum. For the case of our postulated ideal grid transfer operators it also would not matter whether the GS relaxations are applied when going up or going down, only the total number of GS relaxations on each level would count.

To establish the relation between multigrid grid transfer operators and wavelet theory, let us point out a formal similarity. For vanishing d coefficients, the wavelet analysis step is given by (Eq. 26 of ref. [7])

$$s_i^{2h} = \sum_{j=-m}^m \tilde{h}_j s_{j+2i}^h \quad (18)$$

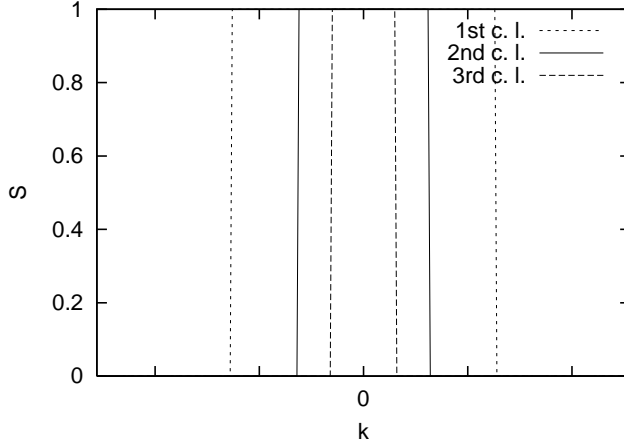


Figure 5: The ideal function $S^l(k)$ defined in (Eq. 16) on three resolution levels denoted by first coarse level, second coarse level and third coarse level. On the zeroth original level the function is identical to one over the entire interval. It gives a perfect dyadic decomposition of the Fourier spectrum.

and is formally identical to a restriction operation. A wavelet synthesis step for the s coefficients is given by (formula 27 of ref. [7])

$$s_{2i}^h = \sum_{j=-m/2}^{m/2} h_{2j} s_{i-j}^{2h} \quad (19)$$

$$s_{2i+1}^h = \sum_{j=-m/2}^{m/2} h_{2j+1} s_{i-j}^{2h} .$$

and is formally identical to a prolongation operation. One can now for example easily see that the injection scheme for the restriction and linear interpolation for the prolongation part corresponds to a wavelet analysis and synthesis steps for 1st order interpolating wavelets. Using the values of the filters \tilde{h} and h for interpolating wavelets we obtain

$$s_i^{2h} = s_{2i}^h \quad (20)$$

and

$$s_{2i}^h = s_i^{2h} \quad (21)$$

$$s_{2i+1}^h = \frac{1}{2} s_i^{2h} + \frac{1}{2} s_{i+1}^{2h} .$$

which is the standard injection and interpolation. As a consequence of the fact that it can be considered as a wavelet forward and backward transformation, the combination of injection and interpolation satisfy the identity property of our ideal grid transfer operator pair, namely that applying a restriction onto a prolongation gives the identity.

Usually injection is replaced by the full weighting scheme,

$$s_i^{2h} = \frac{1}{4} s_{2i-1}^h + \frac{1}{2} s_{2i}^h + \frac{1}{4} s_{2i+1}^h. \quad (22)$$

This scheme has the advantage that it conserves averages, i.e it satisfies the monopole part of the multipole conservation property of an ideal restriction operator. Applying it to a charge density thus ensures that the total charge is the same on any grid level. Trying to put the full weighting scheme into the wavelet theory framework gives a filter \tilde{h} with nonzero values of $\tilde{h}_{-1} = \frac{1}{4}$, $\tilde{h}_0 = \frac{1}{2}$, $\tilde{h}_1 = \frac{1}{4}$. This filter \tilde{h} does not satisfy the orthogonality relations of wavelet theory (formula 8 of ref. [7]) with the h filter corresponding to linear interpolation. Hence a prolongation followed by a restriction does not give the identity.

A pair of similar restriction and prolongation operators that conserve averages can however be derived from wavelet theory. Instead of using interpolating wavelets we have to use lifted interpolating wavelets [15, 16]. In this way we can obtain both properties, average conservation and the identity for a prolongation restriction sequence. Using the filters derived in ref. [7] we obtain

$$s_i^{2h} = -\frac{1}{8} s_{2i-2}^h + \frac{1}{4} s_{2i-1}^h + \frac{3}{4} s_{2i}^h + \frac{1}{4} s_{2i+1}^h - \frac{1}{8} s_{2i+2}^h \quad (23)$$

$$\begin{aligned} s_{2i}^h &= s_i^{2h} \\ s_{2i+1}^h &= \frac{1}{2} s_i^{2h} + \frac{1}{2} s_{i+1}^{2h}. \end{aligned} \quad (24)$$

Let us finally discuss the first property of our postulated ideal restriction operator, namely that it is a perfect low pass filter. Obviously any finite length filter can only be an approximate perfect low pass filter. (Fig 6) shows the S function for several grid transfer operators. One clearly sees that the Full Weighting operator is a poor low pass filter, the filter derived from second degree lifted wavelets is already better and the filters obtained from 10th degree Daubechies wavelets and twofold lifted 6th order interpolating wavelets are best. The Daubechies 6th degree filter is intermediate and of nearly identical quality as the one that is a mixture of the Full Weighting and second degree lifted wavelet filters. In contrast to the former, the later does however not fulfill the identity property.

The degree of perfectness for the frequency separation is also related to the multipole conservation property of our postulated ideal grid transfer operators. As one sees from (Fig. 6) filters which correspond to wavelet families with many vanishing are closer to being ideal for frequency separation than those with few vanishing moments. At the same time the number of vanishing moments determines how many multipoles are conserved when the charge density is brought onto the coarser grids.

The right panel of (Fig. 7) shows the convergence rate of a sequence of V cycles for the full weighting/interpolation (Eq. 22,21) scheme and various wavelet based schemes, namely the scheme obtained from second order lifted wavelets (Eq. 23,24), the corresponding scheme, but obtained from twofold lifted 6-th order wavelets as well as schemes obtained from 6th and 10th order Daubechies wavelets. The numerical values for the filters are listed in the Appendix. One can observe a clear correlation between the convergence rate and the the degree of perfectness of the S function. A high degree of perfectness

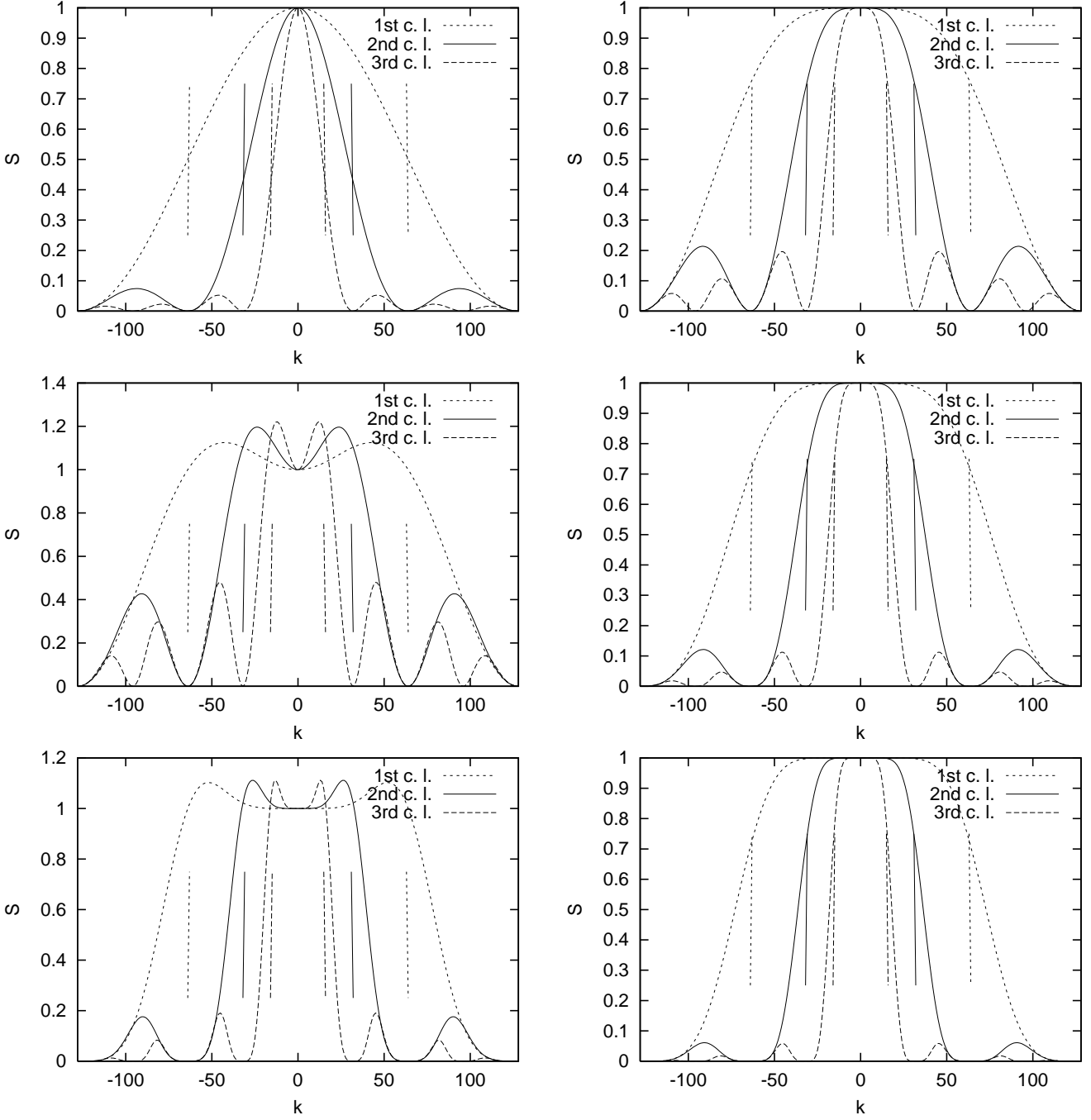


Figure 6: The function $S^l(k)$ defined in Eq. 16 on the coarser resolution levels $Lmax - 1$, $Lmax - 2$ and $Lmax - 3$ (corresponding to grid spacings of $2h$, $4h$ and $8h$ if the finest resolution is h) for several restriction operators: Top left, Full weighting; middle left, 2nd order lifted wavelets, bottom left 6th order twofold lifted wavelets; top right half and half mixture between Full Weighting and 2nd order lifted wavelets; middle right, 6th order Daubechies; bottom right, 10th order Daubechies. S was calculated numerically for an initial data set of 256 points. Hence the allowed values of k in (Eq. 17) range from -128 to 127. The lower half, quarter and eight of the spectrum where the ideal function would switch between the values of 0 and 1 are denoted by vertical lines.

is particularly useful in connection with high order discretizations of the Laplacian. Most of the filters of the grid transfer operators are longer than the standard Full Weighting filter, which just has 3 elements. The lifted 2nd order interpolating wavelet restriction filter has for instance 5 elements and the 6-th degree Daubechies filter 6 elements. This does however not lead to a substantial increase of the CPU time. This comes from the fact that on modern computers the transfer of the data into the cache is the most time consuming part. How many numerical operations are then performed on these data residing in cache has only a minor influence on the timing. The new wavelet based schemes for restriction and prolongation are therefore more efficient than the Full Weighting scheme, both for finite difference discretizations and scaling function basis sets. It is also obvious that the multigrid approach for scaling/wavelet function basis sets is more efficient than the diagonal preconditioning approach.

The identity property for a restriction prolongation operator pair was only necessary for the case of operators where the restriction part is a perfect low pass filter. One might therefore wonder how useful it is in the context of the only nearly perfect filters. The numerical experience suggests that it is nevertheless a useful property. One can for example compare the convergence rates using either the 6-th order Daubechies filters or the filter that is the average of Full Weighting and lifted 2nd order wavelet filters. (Fig. 6) shows that their restriction parts have very similar S functions. Nevertheless we always found a better convergence rate with the Daubechies filter which satisfies the identity property.

For the 2-dimensional Poisson equation it has been shown, that the convergence rate compared to the standard Full Weighting scheme can be improved by tailoring grid transfer operators for the relaxation scheme used [17]. The theoretical foundations for this is furnished by local Fourier analysis [18]. The same approach could certainly also be used for the 3-dimensional case considered here. It is to be expected that the grid transfer operators found by such an optimization would be very close to the ones that we have obtained from wavelet theory.

The main justification for the relaxations in the upper part of the traditional multigrid algorithm shown in (Fig. 4) is to eliminate the high frequencies. This can however be done directly by fast wavelet transformations based on wavelets that have good localization properties in frequency space such as lifted interpolating wavelets. As a consequence the traditional multigrid algorithms can be simplified considerably as shown in (Fig. 8). Using wavelet based restriction and prolongation operators we can completely eliminate the GS relaxation in the first part of the V cycle where we go from the fine grid to the coarsest grid. We baptize such a simplified V cycle a half-way V cycle. The numerical results, obtained with the half-way V cycle, shown in the right hand plots of (Fig. 7), demonstrate that the convergence is slightly faster than for the traditional multigrid algorithm based on the same restriction and prolongation scheme. In addition one step is faster. It is not necessary to calculate the residue after the GS relaxations. Otherwise the number of GS relaxations and restrictions/prolongations is identical in the full and half-way V cycle. On purpose no CPU times are given in this context because optimization of certain routines [19] can entirely change these timings. Because the residue is never calculated in the half-way V cycle, the memory requirements are also reduced.

The number of GS relaxations in the half-way V cycle was chosen to be 4 in order to

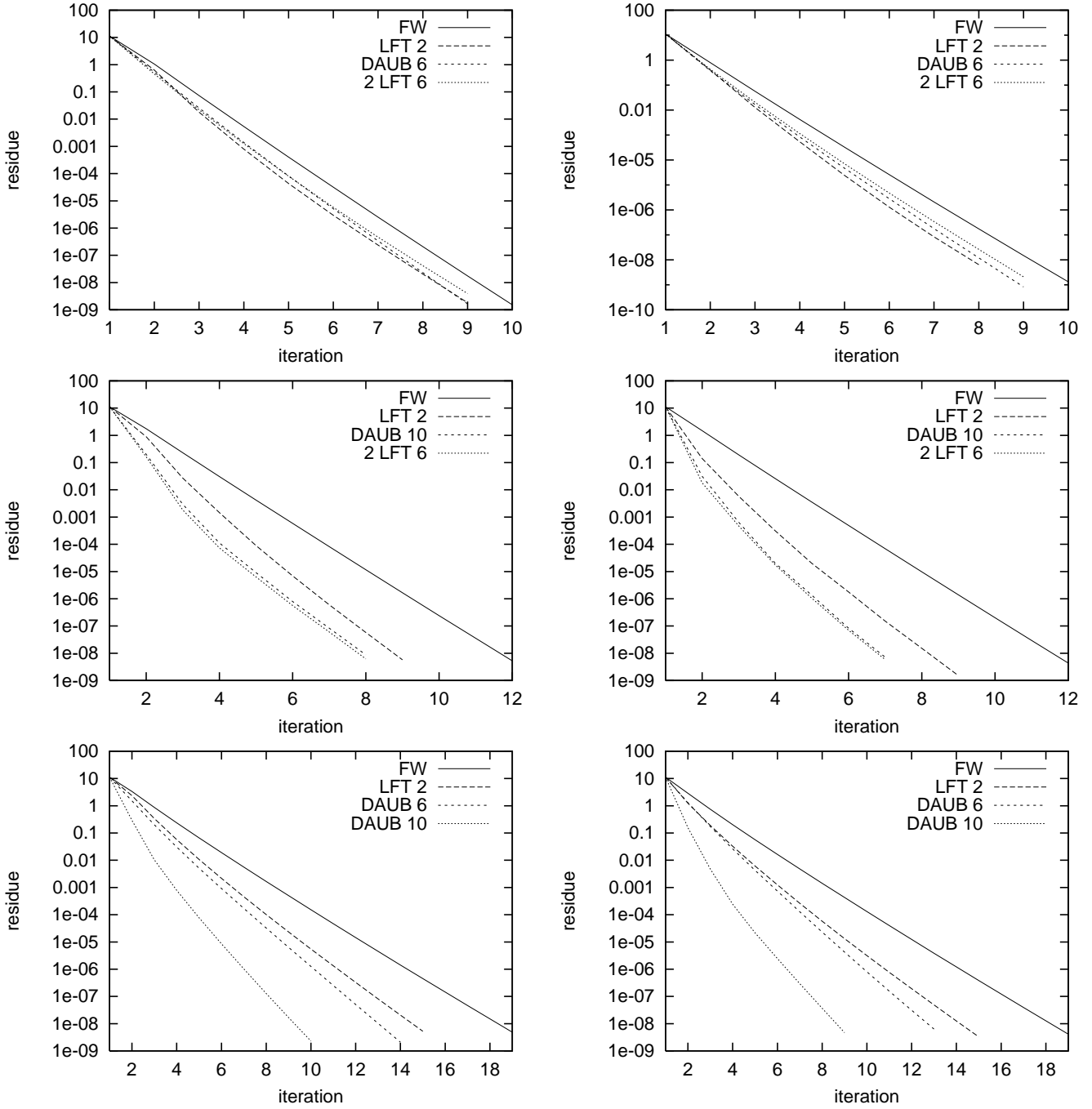


Figure 7: The convergence rate of a sequence of V cycles (left hand side) and halfway V cycles (right hand side). In the upper two plots Poisson's equation was discretized by second order finite differences, In the middle two plots by 6-th order finite differences and in the lower two plots by 6-th order and 10th order (for the case of transfer operators based on DAUB 10) interpolating scaling functions. Shown are results for the Full Weighting scheme (FW) second order lifted wavelets (LFT 2), twofold lifted 6-th order wavelets (2 LFT 6) and 6-th and 10-th order Daubechies wavelets. In the case of ordinary V cycles 2 GS relaxations were done on the finest level both when going up and coming back down, in the case of the halfway V cycle 4 GS relaxation were done on the finest level.

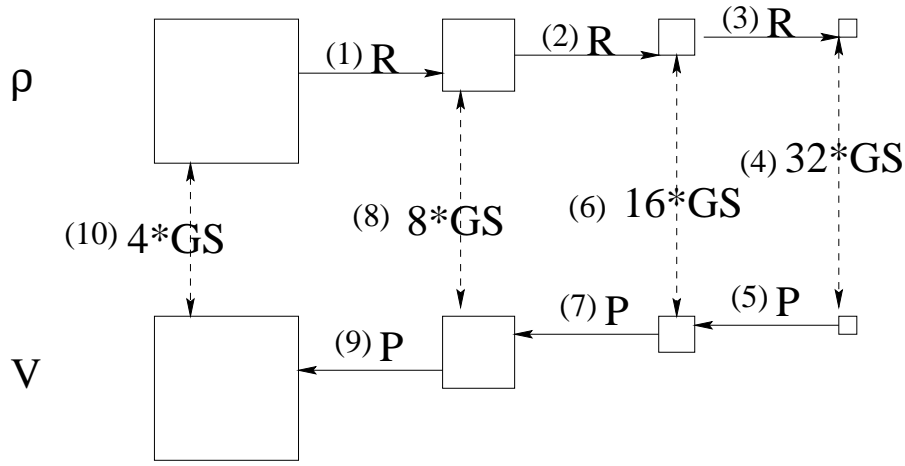


Figure 8: Schematic representation of a halfway V cycle as described in the text. The abbreviations are the same as in (Fig. 4).

allow for an unbiased comparison with the traditional V cycle where also 4 GS relaxations were done on the finest grid level. For optimal overall efficiency putting the number of GS relaxation to 3 is usually best, with the values of 2 and 4 leading to a modest increase in the computing time. The convergence rate of halfway V cycles as a function of the number of GS relaxations on the finest grid level is shown in (Fig 9).

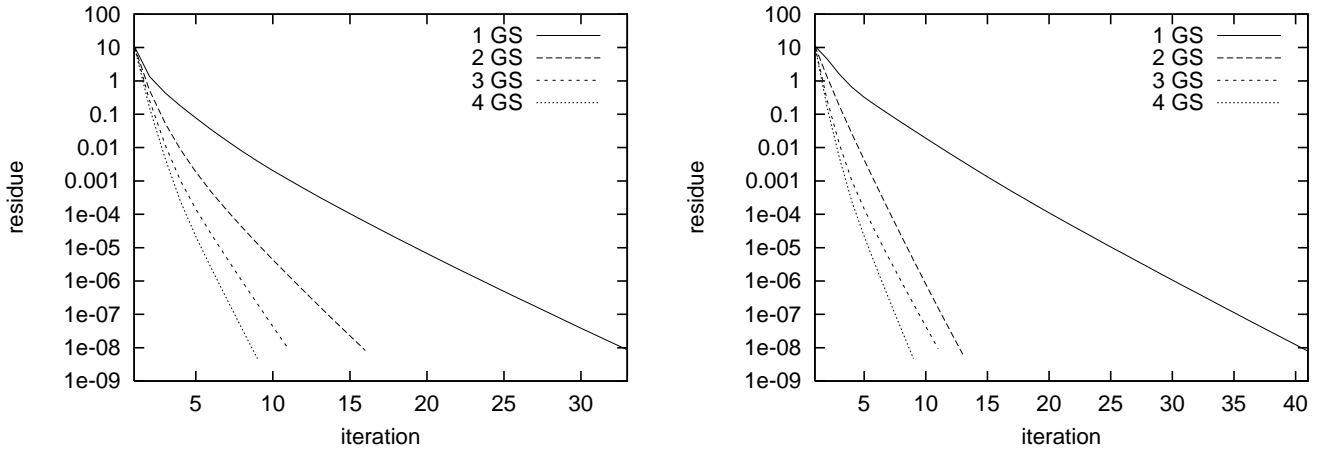


Figure 9: The convergence rate for halfway V cycles with 4, 3, 2 and 1 GS relaxation on the finest grid level. In the left panel 2nd order finite differences were used, in the right panel 6th order finite differences.

In all the previous examples we specified the number of GS relaxations on the finest grid level. On the coarser grid levels the number of iterations was allowed to increase by a factor of two per grid level. In this way it was practically always possible to find the exact solution on the most coarse grid. In addition we found that this trick slightly

reduces the number of iterations and the total CPU time. The overall behavior of all the different methods is however identical when the number of GS relaxation is constant on each grid level.

5 Conclusions

Our results demonstrate that halfway V cycles with the restriction and prolongation steps based on wavelet theory are the most efficient approach for the solution of the 3-dimensional Poisson's equation. It is most efficient both for finite difference discretizations and for the case where scaling functions or wavelets are used as basis functions. We expect that the approach should also be the most efficient one in connection with finite elements. It is essential that the wavelet family used for the derivation of the restriction and prolongation schemes has at least one vanishing moment and conserves thus average quantities on the various grid levels. Wavelet families with more vanishing moments do not lead an appreciable increase of the convergence rate compared to the case of one vanishing moment for low order discretizations of Poissons equation, but lead a modest further increase for high order discretizations. In the case where a wavelet family was used to discretize the Laplace operator, it is best to use the same wavelet family to construct the grid transfer operators. In addition to increased efficiency of the proposed halfway V cycle in terms of the CPU time, it is also simpler than the standard V cycle. This makes not only programming easier, but also reduces the memory requirements.

6 Acknowledgments

I was fortunate to have several discussion with Achi Brandt about this work. His great insight on multigrid methods, that he was willing to share with me, helped a lot to improve the manuscript. I thank him very much for his interest and advice.

7 Appendix

Filter for twofold lifted 6th order interpolating wavelets [21]:

$$\begin{aligned} h_1 &= 75/128, h_3 = -25/256, h_5 = 3/256, \\ \tilde{h}_0 &= 2721/4096, \tilde{h}_1 = 9/32, \tilde{h}_2 = -243/2048, \tilde{h}_3 = -1/32, \\ \tilde{h}_4 &= 87/2048, \tilde{h}_6 = -13/2048, \tilde{h}_8 = 3/8192. \end{aligned}$$

The values for negative indices follow from the symmetry $h_i = h_{-i}$ and $\tilde{h}_i = \tilde{h}_{-i}$.

Filters for 6-th order Daubechies wavelets [4]:

$$\begin{aligned} h_{-2} &= 0.3326705529500826159985d0, h_{-1} = 0.8068915093110925764944d0, \\ h_0 &= 0.4598775021184915700951d0, h_1 = -0.1350110200102545886963d0, \\ h_2 &= -0.0854412738820266616928d0, h_3 = 0.0352262918857095366027d0. \\ \tilde{h}_i &= h_i. \end{aligned}$$

Filters for 10-th order extremal Daubechies wavelets [4]:

$$\begin{aligned} h_{-4} &= .1601023979741929d0, h_{-3} = .6038292697971897d0, \\ h_{-2} &= .7243085284377729d0, h_{-1} = .1384281459013207d0, \end{aligned}$$

$h_0 = -.2422948870663820d0$, $h_1 = -.0322448695846384d0$,
 $h_2 = .0775714938400457d0$, $h_3 = -.0062414902127983d0$,
 $h_4 = -.0125807519990820d0$, $h_5 = .0033357252854738d0$.
 $\tilde{h}_i = h_i$.

References

- [1] A. Brandt, *Mathematics of Computation* **31**, 333 (1977)
- [2] W. Dahmen, in *Acta numerica* Cambridge University Press (1997)
- [3] A. Brandt, Multiscale Scientific Computation: Review 2001, in T. J. Barth, T. F. Chan and R. Haimes (eds.) *Multiscale and Multiresolution Methods: Theory and Applications* Springer Verlag, Heidelberg, 2001; or <http://www.wisdom.weizmann.ac.il/achi/>
- [4] I. Daubechies, *Ten Lectures on Wavelets*, SIAM, Philadelphia (1992)
- [5] W. Dahmen, S. Prössdorf, R. Schneider: *Wavelet approximation methods for pseudo-differential equations II: Matrix compression and fast solution*, *Advances in Computational Mathematics*, **1**, (1993)
- [6] S. Jaffard, *Wavelet methods for fast resolution of elliptic problems* *SIAM J. Numer. Anal.* **29** (1992)
- [7] S. Goedecker: *Wavelets and their application for the solution of partial differential equations*, Presses Polytechniques Universitaires et Romandes, Lausanne, Switzerland 1998, (ISBN 2-88074-398-2)
- [8] S. Goedecker, O. Ivanov, *Comp. in Phys*, **12**, 548 (Nov/Dec 1998)
- [9] S. Goedecker, O. Ivanov, *Sol. State Comm.*, **105** 665 (1998)
- [10] R. A. Lippert, T. Arias and A. Edelman, *J. Comp. Physics*, **140**, 278 (1998)
- [11] T. A. Arias, *Rev. Mod. Phys.* 71, **267** (1999)
- [12] Y. Saad, *Iterative methods for sparse linear systems* , PWS Publishing Company, Boston, (1996)
- [13] U. Trottenberg, C. Oosterlee, A. Schüller, *Multigrid*, Academic Press, San Diego, CA, 2001
- [14] W. Hackbusch and U. Trottenberg, *A Multigrid Method*, Springer, Berlin, 1982 ; W. L. Briggs, Van Emden Henson, S. F. McCormick *A Multigrid Tutorial*, second edition, SIAM, Philadelphia, PA, 2000
- [15] R. Schneider: *Multiskalen- und Wavelet-MatrixKompression*, Teubner publishing, Stuttgart 1998

- [16] W. Sweldens, *Appl. Comput. Harmon. Anal.* **3**, 186 (1996).
- [17] D. Barkai and A. Brandt, *Appl. Math. Comp.* **13** 215 (1983)
- [18] A. Brandt, in Preliminary Proc. 4th Copper Mountain Conf on Multigrid Methods, Copper Mountain, Colorado 1989; A. Brandt, *SIAM J. Num. Anal.* **31** 1695 (1994)
- [19] S. Goedecker, A. Hoisie, *Performance Optimization of numerically intensive codes*, SIAM publishing company, Philadelphia, USA 2001 (ISBN 0-89871-484-2)
- [20] L. Greengard and V. Rokhlin, *J. Comp. Phys.*, **73**, 325 (1987) ; L. Greengard, *Science*, **265**, 909 (1994)
- [21] W. Sweldens, *SIAM Journal on Mathematical Analysis* **29**, 511 (1998).
- [22] G. Deslauriers and S. Dubuc, *Constr. Approx.* **5**, 49 (1989).
- [23] G. Beylkin, *SIAM J. on Numerical Analysis* **6**, 1716 (1992).
- [24] G. Beylkin, R. Coifman and V. Rokhlin, *Comm. Pure and Appl. Math.*